

A Numerical Study on Laminar Free Convection between Vertical Flat Plates with Symmetric Heating

Ameer A. Jadoaa

Assistant lecturer

Electromechanical Eng. Dep.-University of Technology

Abstract

The development of free convection in a viscous fluid between heated plates is investigated. The basic governing continuity, momentum, and energy equations are solved numerically by finite difference method. Results are obtained for the variations of Nusselt number, velocity, temperature, and pressure throughout the flow field assuming the fluid to enter the channel with ambient temperature and a flat velocity profile. The flow and heat-transfer characteristics of the channel are studied and a development height established. Heating plate condition is (C.W.T and C.H.F). An correlation equation has been deduced for the average Nusselt number as a function of Rayligt number. A comparison is made between the results of this theoretical investigation and theoretical work of (Bodoia, J.R 1962)^[1].

Key words: Free Convection, Laminar, constant wall temperature, constant heat flux and, Vertical Plate.

دراسة عددية في التشكيل الطباقي لجريان الحمل الحر لمائع بين صفيحتين عموديتين متناظرة التسخين

الخلاصة

يتضمن هذا البحث التحقيق في دراسة نظرية في تشكيل جريان الحمل الحر في مائع لزج بين صفيحتين عموديتين بواسطة حل معادلات الأستمبرارية، الزخم، ومعادلة الطاقة باستخدام طريقة الفروقات المحددة وحلها عددياً. النتائج المكتسبة لتغير رقم نسلت، السرعة، درجة الحرارة، والضغط في كافة أنحاء مجال الجريان . ويفترض أن المائع الداخل إلى القناة بدرجة حرارة المحيط ومنحنى السرع الأسبيابي. تم دراسة خصائص انتقال الحرارة والجريان المجرى وصفة سرعة التشكيل ظرف التسخين هي فيض حراري متغير مع ثبوت درجة الحرارة وفيض حراري ثابت مع تغير درجة الحرارة. معادلات تجريبية أستنثت لمعدل رقم نسلت دالة لرقم رايلى. أجريت مقارنة بين التحقيق النظري للعمل الحالي والتحقيق النظري لمصدر (Bodoia, J.R 1962)^[1].

الكلمات الدالة:حمل قسري،جريان طباقي،ثبت درجة حرارة السطح،ثبت الفيض الحراري،صفحة عمودية.

Nomenclatures

a: surface conductance defined by equation(14)
 b: half-width of channel
 c: specific heat of fluid
 g: gravitational constant
 h: heat absorbed by fluid from entrance to a particular elevation in channel
 h':heat absorbed by fluid from entrance to channel exit
 k: thermal conductivity of fluid
 p: fluid pressure
 T_1 : temperature of channel walls
 u: fluid velocity in x-direction
 u_0 : fluid velocity at channel entrance
 U: dimensionless velocity in x-direction defined by equation (8)
 v: fluid velocity in y-direction
 V: dimensionless velocity in y-direction defined by equation (8)
 x,y: Cartesian co-ordinate system
 N: Number of grid
 P_o : hydrostatic fluid pressure

Introduction

Several investigations have studied laminar free convection in vertical, parallel-plate channels. All of them, however, have restricted their consideration to either identical heating of the two walls ^[2] or the so-called "fully developed" flow that characterize a channel whose height is large compared to the spacing between the walls ^[3]. The majority of the latter studies ^[4] deal with combined free and forced convection. In the case of vertical tubes, to the present authors' knowledge, all published free convection results, for example, have been for symmetrically heated tubes.^[5] The effect of asymmetric heating in free convection, therefore, has not been fully investigated, although the corresponding problem in forced convection has been quite extensively studied. References for the latter case

p' :pressure defect defined by equation(4)
 P: dimensionless pressure defect defined by equation (8)
 T: fluid temperature
 T_o : ambient temperature
 L: height of channel
 Z: dimensionless height of channel defined by $Z = Gr = 1$
 v: fluid kinematic viscosity
 ρ : fluid density
 ρ_o : fluid density at ambient temperature
 Θ : dimensionless temperature defined by equation (8)
 Gr: Grashoff number defined by equation (9)
 Nu: Nusselt number defined by equation (15)
 X,Y: dimensionless Cartesian co-ordinate system
 β : fluid expansivity defined by equation(7)

are not relevant to the present study and hence will not be listed here.

In a wide class of natural convection processes, heat transfer occurs from a heated vertical surface placed in a quiescent medium at a uniform temperature. If the plate surface temperature is greater than the ambient temperature, the fluid adjacent to the vertical surface gets heated, becomes light and rises. Heavier fluid from the neighboring areas rushes in to take the place of the rising fluid; similarly, the flow for a cooled surface is downwards. The fluid layer in contact with the surface is stationary due to the no-slip condition and the fluid far from the vertical surface is stagnant because of the infinite quiescent medium. A boundary layer flow exists and the region outside the boundary layer is unaffected by the flow ^[6]. Laminar flow exists within the boundary layer up to a certain height of the plate, beyond which turbulence gradually develops

because of the associated thermal instability. In a smooth vertical parallel plate channel that are open to the ambient at top and bottom ends, natural convection occurs when at least one of the two plates forming the channel is heated or cooled. The resulting buoyancy-drive flow can be laminar or turbulent depending on the channel geometry, fluid properties and temperature difference between the plates and ambient. The Rayleigh number at which flow becomes turbulent in vertical channels is different from that of flow over a vertical flat plate. Surface thermal conditions may be idealized as being isothermal or isoflux and symmetrical or asymmetrical. For small aspect ratio (length to inter-plate spacing), independent boundary layer develops at each surface and a condition similar to that of a vertical plate in an infinite quiescent medium takes place. For large aspect ratio, however, boundary layers developed on opposing surfaces eventually merge to yield a fully developed condition. Due to modern application of cooling of electronic equipments such as printed circuit boards, there has been resurgence of interest in studying natural convection in vertical channels. Understanding the flow pattern in this equipment may significantly improve their design and consequently their operational performance^[7]. The effect of other parameters including different forms of heating, transient regimes, chimney effect and channel geometry were investigated by a number of researchers. (Shahin, G. A. and Floryan, J. M)^[8]. Studied the heat transfer enhancement generated by the chimney effect in a system of vertical channels. The increase in heat transfer with adiabatic chimneys was studied numerically and a heat transfer

correlation was presented.^[9] Laminar free convection boundary layer over a vertical flat plate with an exponential variation of surface temperature in viscous fluids is analyzed using the local no similarity method. The present approach takes into consideration the no similarity terms appearing in the momentum and energy equations, which have been unaccounted for previously, in for example, the similarity and the local similarity methods. The governing equations are solved numerically using the Keller-box method, an efficient implicit finite difference scheme. Numerical results are presented in the form of heat transfer rates, local wall shear stress, and velocity and temperature profiles. The heat transfer rates and local wall shear stress obtained show good agreement with available no similar solutions. The effects of various values of transformed stream-wise coordinate (g) and Prandtl numbers on velocity and temperature profiles are also presented. Chalmers and Sweden^[10] studied upward laminar flow in a plate with a constant heat flux thermal boundary condition. Development of radial velocity profiles, radial temperature profiles, mixed-mean to wall temperature differences, Nusselt numbers, and pressure drops were predicted and a comparison between these analyses and the small amount of experimental data available at that time was made. The local Nu correlation given in the section equations, i. e. $Nu_x = 0.0185 Gr_x^{0.4}$ ^[11] This work deals with heat transfer coefficient "h" of a isothermal vertical plate with $H = 0.15$ m. The neighborhoods surfaces influence in that coefficient is aimed with simulation and standard experimentation. A novel technology to measure the heat flux, calling "Tangential Heat Flux meter" is applied

and simulation with a CFD commercial code was performing. Five heat flux meters was glued on the vertical plate, heated 20°C over the air temperature. The neighborhoods and air temperature was maintained constants. The distance between the plate and base wall (floor) was changed as well as the distance between the plate and back side wall. Through simulation results will be comparing with experimental. The result expected is a increasing of heat transfer coefficient, very usefully in heat exchange devices. The present study concerns a theoretical investigation of the laminar free convection in air in a parallel-plate vertical flat duct. The duct walls are individually heated uniformly or maintained at constant temperature. The wall heat fluxes or wall temperatures, however, need not be the same practical application of free convection in vertical channels with asymmetric heating of this nature may be found in modern communication equipment. In such equipment, vertical circuits cards containing heat generating electronic devices are arrayed to from vertical channels, and are cooled by free convection.

Equation Analysis

The flow geometry under investigation is as shown in Fig.1. A vertical channel is formed by two parallel plates of height z and infinite width, separated by a distance $2b$. The plates are maintained at a uniform temperature T_1 which exceeds ambient temperature T_o . Fluid rises between them by natural convection and is assumed to enter the channel at T_o with a flat velocity profile u_o . For moderate differences between T_1 and T_o , the flow is governed by the so-called "incompressible natural convection equation"^[1] expressing conservation of mass, momentum, and

energy. The equations are:

$$\frac{\partial u}{\partial x} + \frac{\partial v}{\partial y} = 0 \quad \dots \dots \dots \quad (1)$$

$$u \frac{\partial u}{\partial x} + v \frac{\partial u}{\partial y} = \dots \quad (2)$$

$$v \frac{\partial^2 u}{\partial y^2} - \frac{1}{\rho} \frac{dp}{dx} - g \\ u \frac{\partial T}{\partial x} + v \frac{\partial T}{\partial y} = \frac{k}{\rho c} \frac{\partial^2 T}{\partial^2 y^2} \dots \dots (3)$$

It is customary to express the body force in terms of a buoyancy force define:

Where p_o is the pressure which would obtain at a particular elevation in the channel if the temperature were uniform at T_o throughout the flow field. Noting that:

Equation (2) can be written:

$$u \frac{\partial u}{\partial x} + v \frac{\partial u}{\partial y} = v \frac{\partial^2 u}{\partial y^2} - \frac{1}{\rho} \frac{dp}{dx} + \beta g (T - T_o) \quad \dots \dots \dots (6)$$

Where β is the expansivity of the fluid defined by:

The abovementioned variables and coordinates can be oriented by the following substitutions in accordance^[1].

$$\left. \begin{aligned} U &= \frac{b^2 u}{L \nu G r} \\ V &= \frac{b V}{\nu} \\ X &= \frac{x}{L G r} \\ Y &= \frac{y}{b} \\ P &= \frac{P b^4}{\rho^2 z^2 \nu^2 G r^2} \\ \theta &= \frac{T - T_o}{T_1 - T_o} \end{aligned} \right\} \dots\dots\dots(8)$$

Where Gr is a Grashoff number defined by:

$$Gr = \frac{g\beta(T_1 - T_o)b^4}{Lv^2} \dots \dots \dots (9)$$

Equations (1),(6),and (3) can be placed in dimensionless form writing:

$$U \frac{\partial U}{\partial X} + V \frac{\partial U}{\partial Y} = \frac{\partial^2 U}{\partial Y^2} - \frac{dP}{dX} + \theta \quad \dots \dots \dots \quad (11)$$

$$U \frac{\partial \theta}{\partial X} + V \frac{\partial \theta}{\partial Y} \\ = \frac{1}{\Pr} \left(\frac{\partial^2 \theta}{\partial Y^2} \right) \dots \dots \dots \quad (12)$$

Where Pr , the Prandtl number, defined by:

$$\Pr = \frac{cv\rho}{k} \dots \quad (13)$$

An average surface conductance over the channel height can be defined by:

Where h' is the value of h at $x=z$ if a Nusselt number is defined by:

It is seen upon substitution from equations (13) and (14) to be given by:

$$Nu = \frac{h' \Pr{yk}}{L(T_l - T_e) c_v \rho} \quad \dots \dots \dots (16)$$

The heat transfer coefficient can be calculated as follows:

Hence, the Nusselt number becomes

$$Nu = \frac{hL}{\kappa} = -\frac{\partial t}{\partial y} \frac{L}{T_1 - T_o} = \frac{-\partial \theta}{\partial Y} \dots \dots \dots (19)$$

Mean Nusselt number

A $\frac{1}{3}$ rd Simpsons rule integration is used to evaluate eq(20):

The pressure calculation from equation below:

$$P = P_o + \frac{1}{2} \rho v^2 \quad \dots \dots \dots \quad (22)$$

The boundary conditions in equations (10), (11), and (12) are:

$$\left\{ \begin{array}{l} \text{for } X = 0 \text{ and } 0 \leq Y < 1, \\ U = 0, V = 0, \theta = 0, P = 0 \\ \text{for } Y = 0 \text{ and } X \geq 0; \frac{\partial U}{\partial Y} = 0 \\ , V = 0, \frac{\partial \theta}{\partial Y} = 0 \\ \text{for } Y = 1 \text{ and } X \geq 0; U = 0 \\ , V = 0, \theta = 1 \\ \text{for } Y = 1 \text{ and } X \geq 0; U = 0, \\ V = 0, \theta = \theta(2, N_1) + dy \\ \text{for } X = 0, \text{ and } X = L; \\ P = 0, U = 0 \end{array} \right\} \dots\dots(23)$$

The numerical procedure used in solving these equations subject to their boundary conditions is described in the following:

Numerical Solution

Writing equations (10),(11),(12) in finite difference form and applying

them to the j,k mesh point of a rectangular grid superimposed on the half-channel flow field (Fig.2), there results:

$$\frac{U_{j+1,k+1} + U_{j+1,k} - U_{j,k+1} - U_{j,k}}{\Delta X} + \frac{V_{J+1,K+1} - V_{J+1,K}}{\Delta Y} = 0 \dots \dots \dots (24)$$

Where n is as shown in Fig.(2)

This system of difference equations has been shown^[12] to be a consistent and stable representation of the incompressible natural convection equation.

The solution procedure is as follows: First, values for P_r are selected. Then, beginning at the $j=0$ row (the channel entrance), equation (19) and (20) are applied to the points $k=0,1,2,\dots,n$. There results $2n+3$ equations and the same number of unknowns ($U_{1,0}; U_{1,1}; \dots; U_{1,n}; \Theta_{1,0}; \Theta_{1,1}; \dots; \Theta_{1,n}; P_1$) where symmetry with respect to the x -axis has been noted. After these equations are solved, $V_{1,1}; V_{1,2}; \dots; V_{1,n}$ can be computed from equation (18) where it has been noted that $V_{1,0}=0$. It is now possible to repeat the procedure for the $j=1$ row. Thus advancement row by row up the half-channel can be executed.

For the solution of the simultaneous equations associated with each row a matrix inversion technique was employed which involves a special

from of the Gaussian elimination scheme^[13]. The calculation were performed on a high speed digital computer and for improved accuracy a larger number of mesh points were used in rows near the channel entrance than in those farther up the channel.

The flow in half of the duct is calculation and explicit finite difference technique computer program written in fortran 90 is used and run on Pentium 4 computer. The flow chart of this program is shown in Fig.(24).

Results and Discussion

Variation of mean Nusselt number shown in Fig.(3&4), respectively, for difference Prantl number for constant wall temperature and heat flux . All of the curves have a convergent value 35.7 at $z=4.5 \times 10^{-3}$, which agrees with the analytical result of eq(16).

Variation of local Nusselt number is shown in Fig.(5&6), respectively, for difference Prantl number for constant wall temperature and heat flux . From this, it is noted that all the curves converge to 35.9 independently of Pr , as $z \rightarrow \infty$, whose convergent value is closely related to $\text{Pr}=0.1$ result for a forced convection flow.

Variation of mean Nusselt number with Raylight number shown in Fig.(7,8 & 9),respectively, and comparison between present work and reference^[1] .It can be noted that the average Nusselt number increases with the increase of Rayleigh number.To study the influence of Rayleigh number on the flow field and heat transfer characteristics, the vertical velocity and temperature profiles as well as the isotherms are presented for different Rayleigh numbers.The discrepancy between the present work and ref.^[1] may be attributed to present work errors

or due to difference between the present work actual and ref.^[1] assumption. More of the studies reveals that the difference between the work and another reference tow values is not a strange matter, but the strange becomes from how big is this difference and its effect on the practical applications. The general correlation will be obtained from previous figures as follows:

$$Nu_m = 25.65 Ra^{0.00342} \quad \dots \dots \dots \quad (27)$$

C.W.T Pr=0

$$Nu_m = 30.46 Ra^{0.00456} \quad \dots \dots \dots \quad (28)$$

C.H.F Pr=0

Num. 32.551a

$$Nu_m = 33.37 Ra^{0.00999} \quad \dots \dots \dots \quad (30)$$

NaIII-55.57 Kα
C H F Pr≡

$$Nu_m = 34.59 Ra^{0.00457} \quad \dots \dots \dots \quad (31)$$

Num=34.59Ra
C,W,T Pr='

$$N_{\text{Nu}_m} = 35.24 Ra^{0.00677} \quad \dots \dots \dots \quad (32)$$

$Nu_m = 55.2 + Ra$

C.H.F. PI-7 The developing of temperature

The developing of temperature profiles along the vertical plate are shown in Fig.(10 to 15) for Pr 0.1, 1, 7 for C.W.T and C.H.F respectively .The figure depicted a steep temperature gradient near the heated surface and the thickness of the thermal boundary layer gradually increases as the flow moves from plate inlet toward plate exit. It can be seen that there is relatively high temperature variation near the heated surface causing an appreciable density change, which creates a rapid growth of thermal boundary layer with the plate length.

Developing of velocity profile along the plate axis, for $\text{Pr} = 0.1, 1, 7$ for C.W.T and C.H.F is shown in Fig.(16 to 21) respectively. Profiles reveal the limitation of buoyancy effect at the entrance, and all the profiles show similar distribution about the centerline of the plate. That means the maximum velocity occurs at the plate core.

Figures (22 & 23) shows

representative pressure levels as a function of axial position for constant wall temperature and constant heat flux, respectively. In either case the point at which the pressure defect returns to zero defines the dimensionless plate length which in turn establishes the modified Grashof number. It is noted from this that every curve converges. When $\text{Pr} < 1$, it converges at $z = 10^{-2}$, while $\text{Pr} > 1$ at the greater z , the large Pr is. Since this phenomenon is associated with the entrance lengths.

Conclusions

The following point has concluded:

1. The mean Nusselt number converges, for uniform wall temperature, to 35.7 while for uniform heat flux it converged to 44.3.
 2. The average Nusselt number increases with the increase of Rayleigh number for the same Prantl number.
 3. The effect of buoyancy is small at the plate entrance and increases in the flow direction.
 4. The temperature profile along the plate shows a steep profile near the heated surface with the thermal boundary layer thickness increases as the heat flux increases, for the same axial position.
 5. There is little change in the velocity profile at the plate entrance and the profile bias slightly toward the heated surface at the plate exit. The bias of the profile happens earlier and faster as the heat flux increases.

References

1. Bodoia,J.R .and Osterle,J.F, "The development of free convection between heated vertical plates" j. heat transfervol70, no1, and p.p30-40 (1962).
 2. W.henhaas,"Heat dissipation of parallel plate by free convection"

- vo150, no3, p.p10-30 (1962).
3. S.ockach, "Combined natural and forced convection laminar flow and heat transfer of fluids with and without heat sources in channels with varying wall temperature" asme paper no50p.p15-35 (1980).
 4. L.P.davis and I.J.prona]"Developing of free convection flow of a gas in a heated vertical open tube" j heat mass transfer 14-889-903 (1971).
 5. Rodigro , Douglas and Jose,"Natural convection on vertical flat plate numerical an experimental stud" Universidade de brasilia-departamento de engenharia mecanica-70910-900-df (2003).
 6. Bejan, A."Convection Heat Transfer" Second Edition, Jon Wiley and Sons,Inc (1995).
 7. Incropera, F. P. and DeWitt, D. P."Fundamentals of Heat and Mass Transfer",Fourth Edition, Jon Wiley and Sons (1996).
 8. Shahin, G. A. and Floryan, J. M"Heat Transfer Enhancement Generated by the Chimney Effect in Systems of Vertical Channels". ASME *Journal of Heat Transfer*, Vol. 121, pp. 230-232, (1999).
 9. Lok Yian Yian & Norsarahaida Amin "Local Nonsimilarity Solution for Vertical Free Convection Boundary Layers" Department of Mathematics Universiti TeknologiMalaysia,81310 UTM Skudai, Johor, Malaysia Matematika, Jilid 18, bil. 1, hlm. 21–31 (2002).
 10. Chalmers, Sweden,"Report on a CFD study of natural convection on a vertical plate and CFD simulation of a tunnel fire" A report in MTF112, Convective Heat Transfer (2005).
 11. Rossano Comunelo & Saulo Güths,"Natural convection at isothermal vertical plate neighbourhood influence" 18th International Congress of Mechanical Engineering, Ouro Preto, MG (2005).
 12. R.k.hanna and Manna", An analytical investigation of natural convection in vertical channels" asme paper no67p.p67-80 (1967).

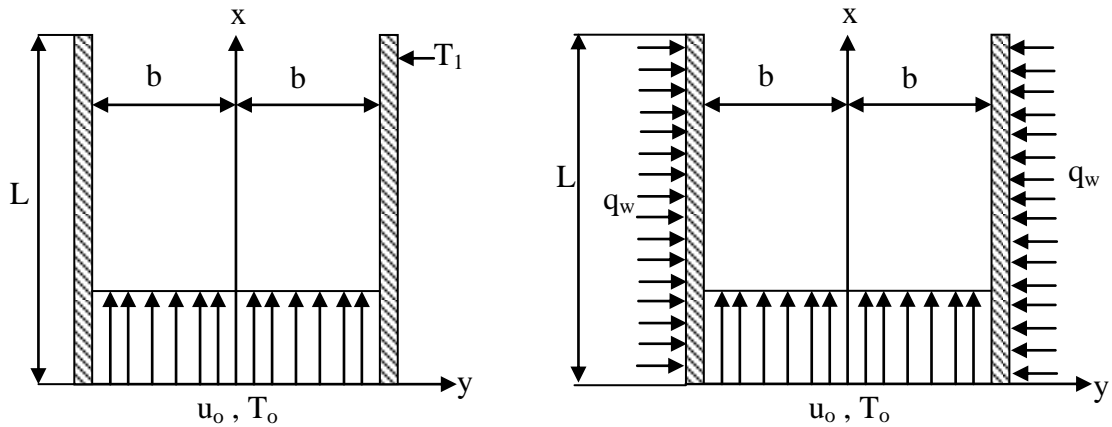


Fig.(1) Configuration of flow

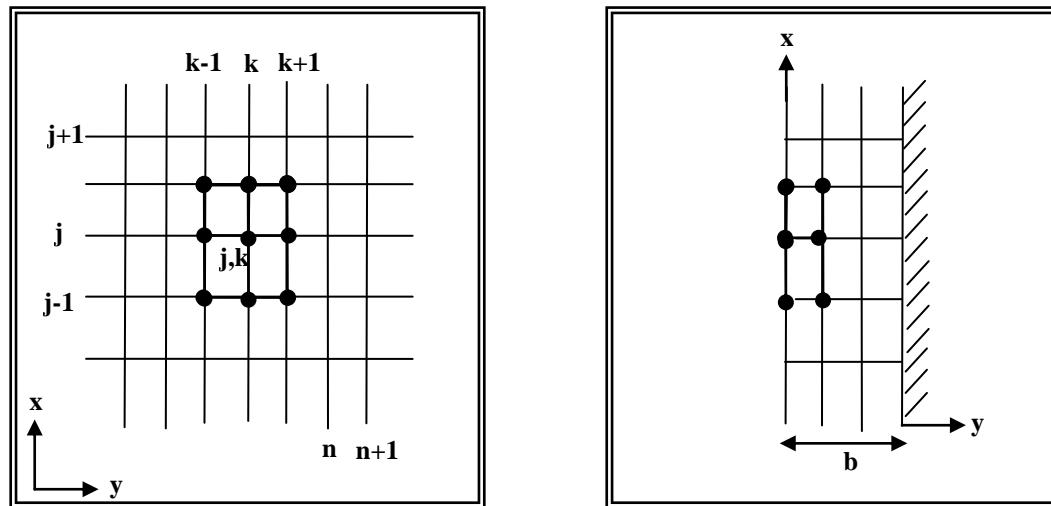


Fig.(2) Mesh network for difference representations

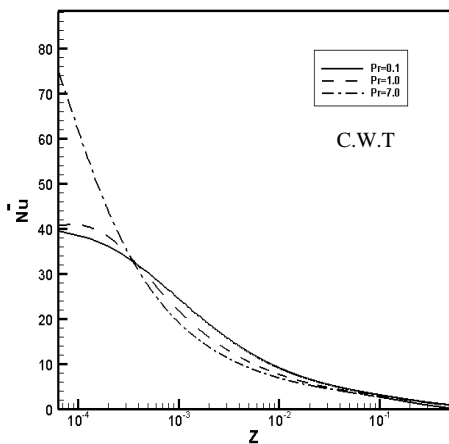


Fig.(3):Mean Nusselt number Versus Dimensionless Height of Channel for Various prandtl number, (C.W.T)

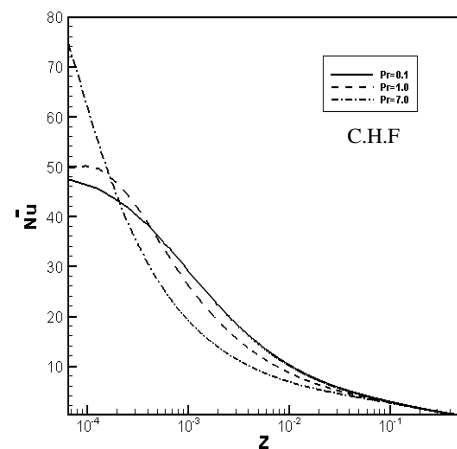


Fig.(4):Mean Nusselt number Versus Dimensionless Height of Channel for Various prandtl number, (C.H.F)

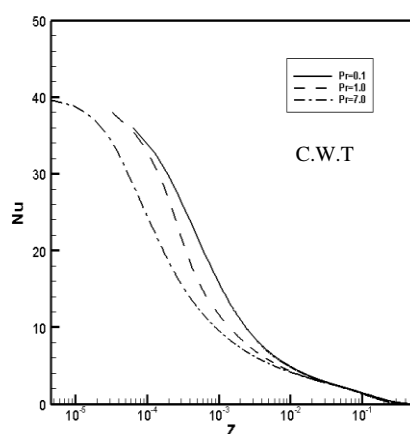


Fig.(5):Local Nusselt number Versus Dimensionless Height of Channel for Various prandtl number, (C.W.T)

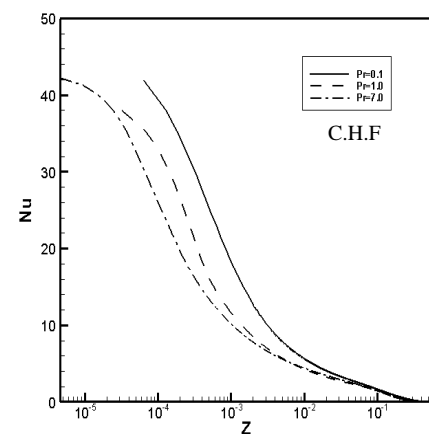


Fig.(6):Local Nusselt number Versus Dimensionless Height of Channel for Various prandtl number, (C.H.F)

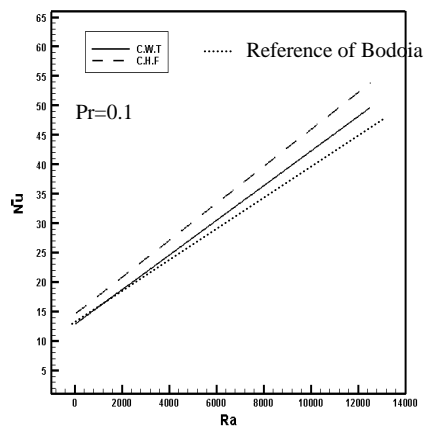


Fig.(7):Mean Nusselt number Versus Raylight number for $Pr=0.1$ for (C.W.T &C.H.F) and Comparison Between Present Work and ref.[

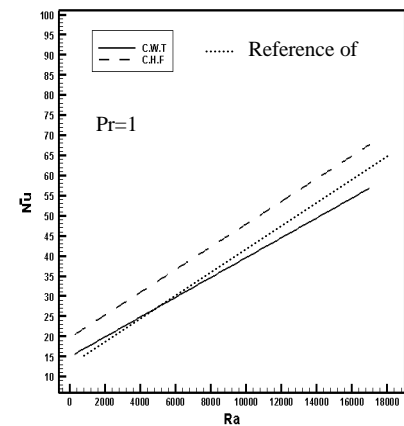


Fig.(8):Mean Nusselt number Versus Raylight number for $Pr=1$ for (C.W.T &C.H.F) and Comparison Between Present Work and ref.[

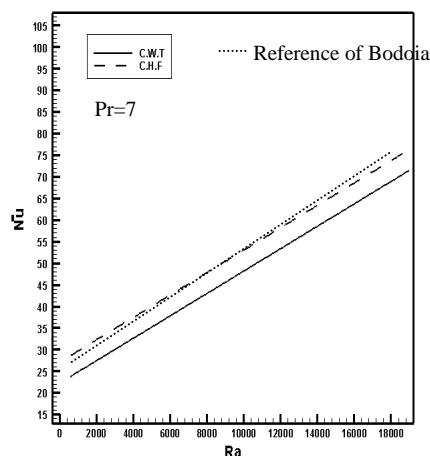


Fig.(9):Mean Nusselt number Versus Raylight number for $Pr=1$ for (C.W.T &C.H.F) and Comparison Between Present Work and ref.[

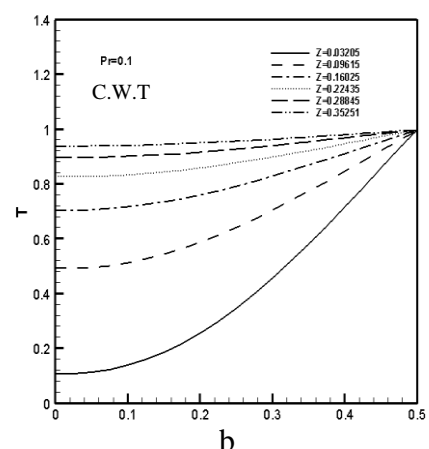


Fig.(10):Developing of Temperature Versus half-width of channel for Versus Dimensionless Height of Channel for $Pr=0.1$ for (C.W.T)

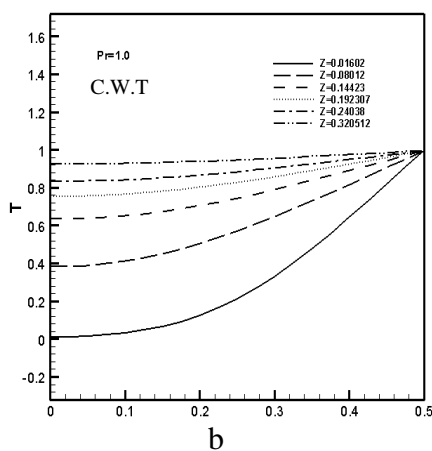


Fig.(11):Developing of Temperature Versus half-width of channel for Versus Dimensionless Height of Channel for $Pr=1$ for (C.W.T)

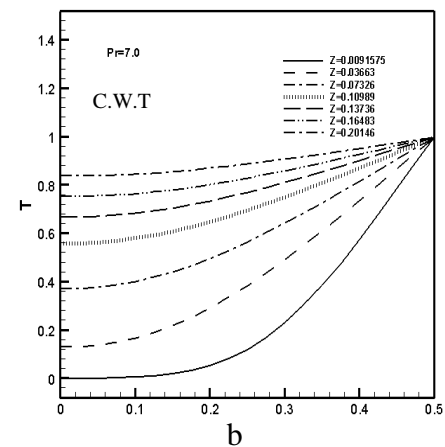


Fig.(12):Developing of Temperature Versus half-width of channel for Versus Dimensionless Height of Channel for $Pr=7$ for (C.W.T)

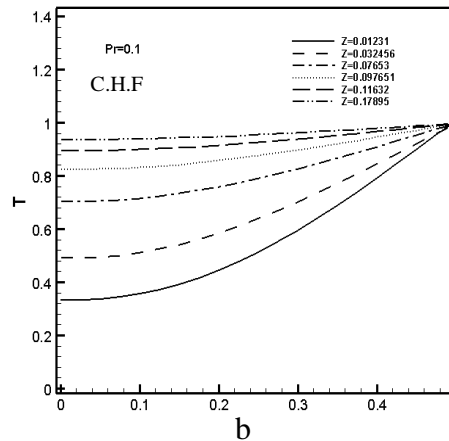


Fig.(13):Developing of Temperature Versus half-width of channel for Versus Dimensionless Height of Channel for $Pr=0.1$ for (C.H.F)

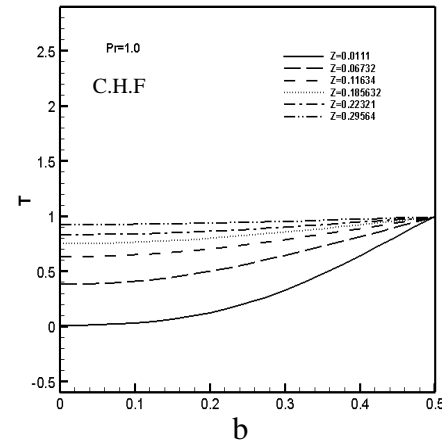


Fig.(14):Developing of Temperature Versus half-width of channel for Versus Dimensionless Height of Channel for $Pr=1$ for (C.H.F)

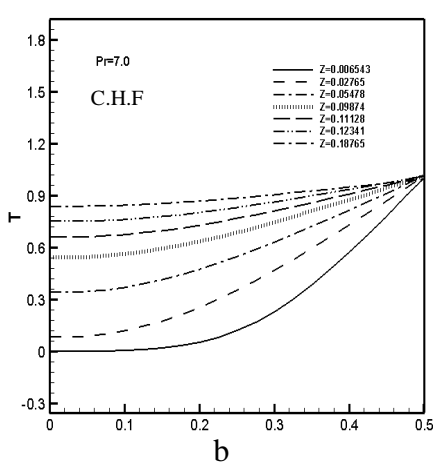


Fig.(15):Developing of Temperature Versus half-width of channel for Versus Dimensionless Height of Channel for $Pr=7$ for (C.H.F)

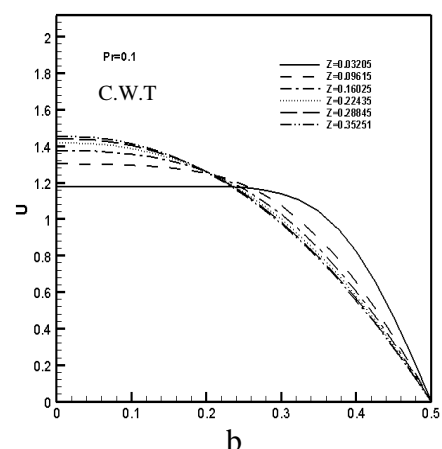


Fig.(16):Developing of Axial Velocity Versus half-width of channel for Versus Dimensionless Height of Channel for $Pr=0.1$ for (C.W.T)

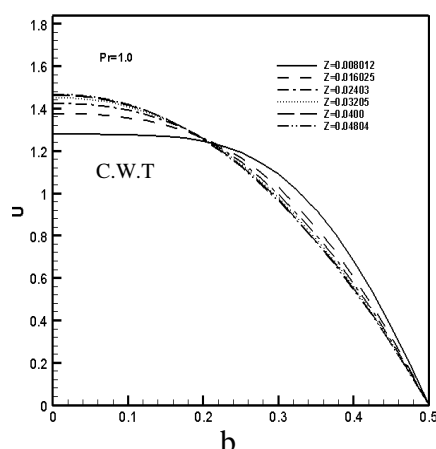


Fig.(17):Developing of Axial Velocity Versus half-width of channel for Versus Dimensionless Height of Channel for $Pr=1$ for (C.W.T)

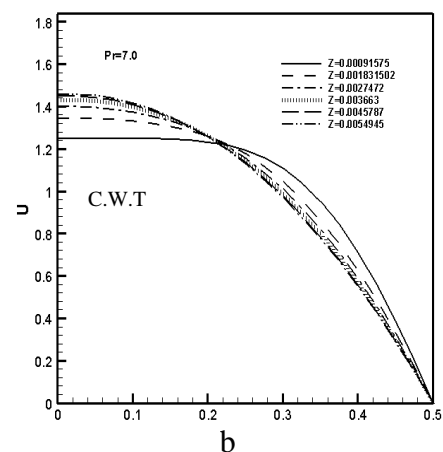


Fig.(18):Developing of Axial Velocity Versus half-width of channel for Versus Dimensionless Height of Channel for $Pr=7$ for (C.W.T)

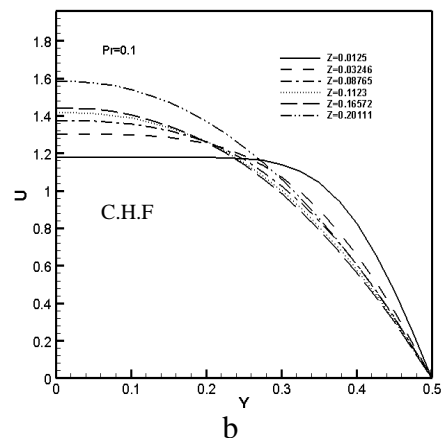


Fig.(19):Developing of Axial Velocity Versus half-width of channel for Versus Dimensionless Height of Channel for $Pr=0.1$ for (C.H.F)

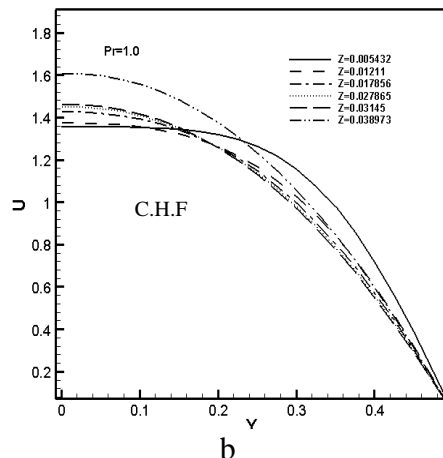


Fig.(20):Developing of Axial Velocity Versus half-width of channel for Versus Dimensionless Height of Channel for $Pr=1$ for (C.H.F)

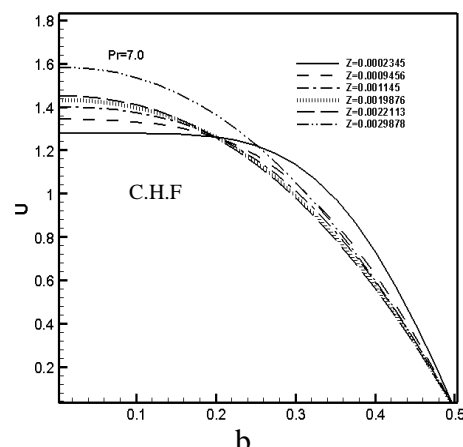


Fig.(21):Developing of Axial Velocity Versus half-width of channel for Versus Dimensionless Height of Channel for $Pr=7$ for (C.H.F)

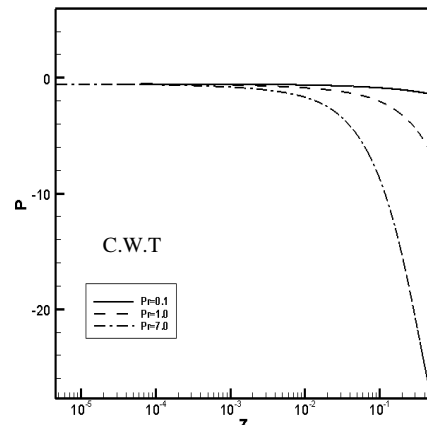


Fig.(22):Pressure Distrbution Versus Dimensionless Height of Channel for Various prandtl number, (C.W.T)

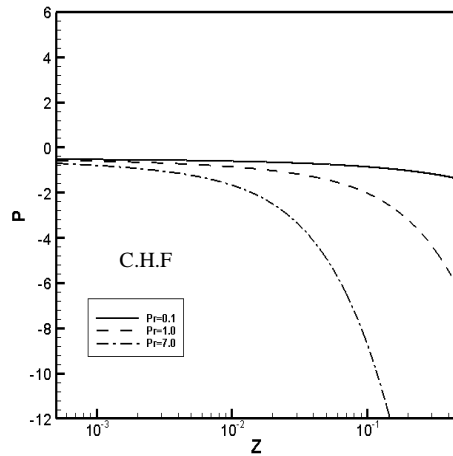


Fig.(23):Pressure Distrbution Versus Dimensionless Height of Channel for Various prandtl number, (C.H.F)

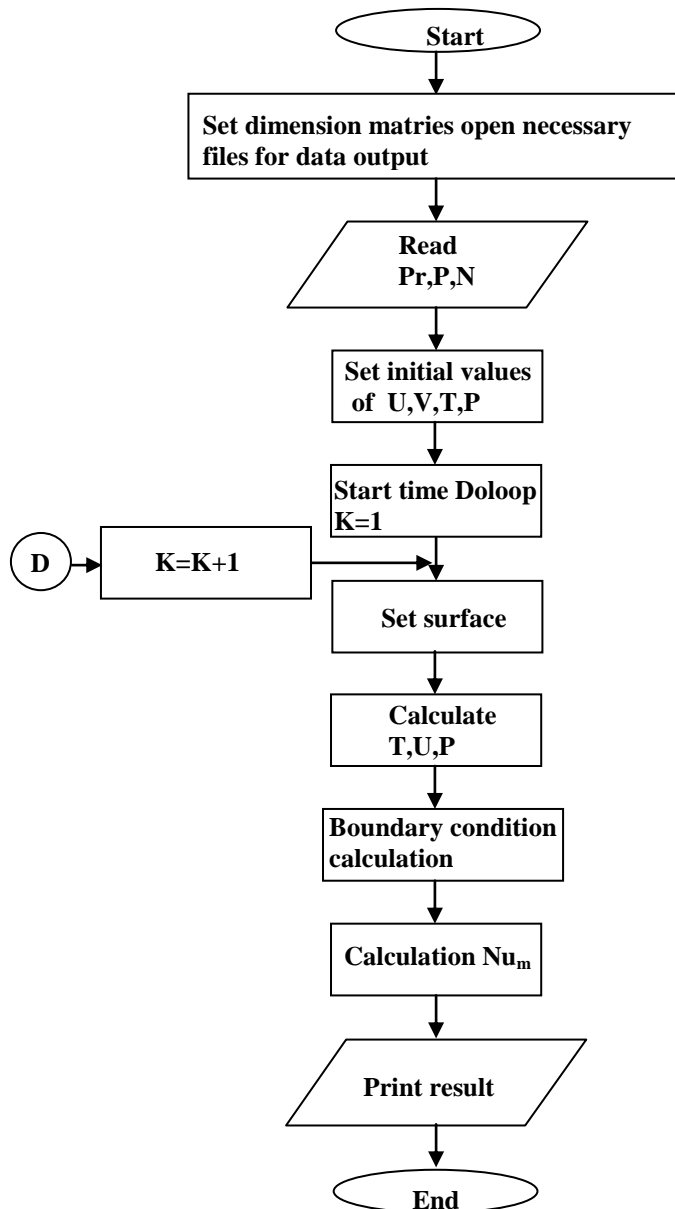


Fig. (24): Flow chart